Federal Aviation Administration

DOT/FAA/AM-07/13
Office of Aerospace Medicine
Washington, DC 20591

Assessment of Injury Potential in Aircraft Side-Facing Seats Using the ES-2 Anthropomorphic Test Dummy

Richard DeWeese
David Moorcroft
Civil Aerospace Medical Institute
Federal Aviation Administration
Oklahoma City, OK 73125

Tom Green
AmSafe Aviation
Phoenix, AZ 85043

M.M.G.M. Philippens
TNO Defense, Security and Safety
2600 JA Delft
The Netherlands

May 2007

Final Report

NOTICE

Technical Report Documentation Page

1. Report No.	2. Government Accession No.	3. Recipient's Catalog No.
DOT/FAA/AM-07/13		

4. Title and Subtitle	5. Report Date
Assessment of Injury Potential in Aircraft Side-Facing Seats Using the ES-2 Anthropomorphic Test Dummy	May 2007
	6. Performing Organization Code

7. Author(s)	8. Performing Organization Report No.
DeWeese RL,[1] Moorcroft DM,[1], Green T,[2] Philippens MMGM[3]	

9. Performing Organization Name and Address		10. Work Unit No. (TRAIS)
[1]FAA Civil Aerospace Medical Institute P.O. Box 25082 Oklahoma City, OK 73125	[2]AmSafe Aviation Phoenix, Ariz. 85043 [3]TNO Defense, Security, & Safety The Netherlands	11. Contract or Grant No.

12. Sponsoring Agency name and Address	13. Type of Report and Period Covered
Office of Aerospace Medicine Federal Aviation Administration 800 Independence Ave., S.W. Washington, DC 20591	14. Sponsoring Agency Code

15. Supplemental Notes

Work accomplished under approved Task: PSRLAB.AV9100

16. Abstract

A project was conducted to assess the injury potential of current side facing aircraft seat configurations using the ES-2 Anthropomorphic Test Dummy proposed for use in Federal Motor Vehicle Safety Standards. The ability of inflatable restraint systems to mitigate injuries in these configurations was also assessed. Impact sled tests were conducted at the Federal Aviation Administration's Civil Aerospace Medical Institute using a side-facing sofa fixture with cushion construction representative of current business jets. The tests simulated three typical seating configurations: occupant in the middle seat, occupant seated next to a rigid wall, and occupant seated next to an armrest end closure. Two types of restraints were evaluated: a three-point body centered conventional restraint with inertia reel and a similar restraint incorporating a new inflatable shoulder restraint (airbag). The test conditions were the 16g, 44 ft/s, horizontal impact specified in 14 CFR 25.562 but without yaw. Test setup techniques were developed to ensure consistent occupant positioning. Test repeatability was assessed for some test conditions.

The suitability of the ES-2 for use in aircraft seat testing was evaluated. Injury criteria were calculated from the data gathered during the tests, including criteria currently published in the Federal Aviation Regulations and Federal Motor Vehicle Safety Standards such as the Head Injury Criteria, upper torso restraint loads, Thoracic Trauma Index, and peak lateral pelvis acceleration. Other research criteria and those identified in proposed Federal Motor Vehicle Safety Standards were also calculated. These criteria included neck forces and moments, Preliminary Lateral Nij, Viscous Criteria, rib deflection, abdominal forces, pubic force, upper spine acceleration, and femur torsion. Results were analyzed to identify criteria relevant for aviation use and seating and restraint system configurations that indicated potential improvements in occupant protection for side-facing seats.

17. Key Words	18. Distribution Statement
Injury Criteria, ES-2, Side Facing Seat, FMVSS No. 214, Aircraft Seat Tests, Inflatable Restraint	Document is available to the public through the Defense Technical Information Center, Ft. Belvior, VA 22060; and the National Technical Information Service, Springfield, VA 22161

19. Security Classif. (of this report)	20. Security Classif. (of this page)	21. No. of Pages	22. Price
Unclassified	Unclassified	30	

Form DOT F 1700.7 (8-72) Reproduction of completed page authorized

ACKNOWLEDGMENTS

The Authors acknowledge the companies that contributed to the side-facing seat configuration survey. Providing data were BE Aerospace, Cessna Aircraft, and DeCrane Aircraft. The information they provided was invaluable during design of the test protocol and contributed toward the validity of the results.

We also thank BE Aerospace for providing the representative aircraft seat cushions used in the tests.

Assessment of Injury Potential in Aircraft Side-Facing Seats Using the ES-2 Anthropomorphic Test Dummy

INTRODUCTION

Dynamic testing and occupant injury assessment have been required for seats in newly certified aircraft since the adoption of Title 14 of the Code of Federal Regulations (CFR) Part 25, 25.562, and similar regulations in Parts 23, 27, and 29 (1). The occupant injury criteria contained in those regulations are primarily focused on protecting the occupant from forward and vertical impacts. Since the biomechanics of side impacts differ significantly from forward or vertical impacts, research was conducted in 1998 to assess injury risk using available side-facing Anthropomorphic Test Dummies (ATDs). The ATDs evaluated included the U.S. Side Impact Dummy (SID), used for U.S. auto safety compliance tests, the Euro-SID 1, used for European Union auto safety compliance tests, and the BioSID, an advanced research dummy (2). Results of this research were used as the basis of Federal Aviation Administration (FAA) policy concerning certification of side-facing seats (3). The aviation industry used the research findings as a guide for seat designs intended to mitigate injury. Recent auto safety research has yielded a better understanding of the biomechanics of side impact (4). Based on this research, the National Highway Traffic Safety Administration (NHTSA) issued a Notice of Proposed Rulemaking (NPRM) to use ES-2re 50% male-size ATD and the SID-IIsFRG 5% female-size ATD and their associated injury criteria to assess new car safety (5). The ES-2re is an improved version of the Euro-SID 1, and the SID-IIsFRG is a scaled down version of the BioSID.

EVALUATION OF IMPROVED SIDE-IMPACT PROTECTION REQUIREMENTS

Current and Proposed Testing Requirements

Recent biomechanical research has resulted in a better understanding of how to quantify the injury risks associated with side impacts in automobiles. These findings were used to develop advanced test dummies and associated injury criteria. Table 1 summarizes the ATDs and injury criteria referenced in current and proposed U.S. Federal Motor Vehicle Safety Standards, current European Union regulations, and current FAA regulations and policy guidance. Current FAA policy also requires that there be no significant body-to-body contact between occupants of a multiple-place seat.

Project Goals

To support FAA policy making activities, a project was conducted by the FAA Civil Aerospace Medical Institute (CAMI) using the ES-2 ATD to evaluate the injury risk presented by a typical side-facing couch configuration

Table 1 - Current and Proposed Side Facing Injury Criteria

Body Region	EU 96/27/EC	FMVSS-208		FMVSS-214	FMVSS-214 Proposed		FAA Policy
	EuroSID 1	HIII 50M	HIII 5F	US SID 50M	ES-2re 50M	SID-IIsFRG 5F	US SID 50M
Head	HPC = 1000	HIC15 = 700	HIC15 = 700	NA	HIC36 = 1000	HIC36 = 1000	HIC = 1000
Neck	NA	Nij =1 T = 937 lb C= 899 lb	Nij =1 T = 589 lb C= 567 lb	NA	NA	NA	NA
Chest	D = 42 mm V*C = 1.0 m/s	Chest Ax = 60 g D = 63 mm	Chest Ax = 60 g D = 52 mm	TTI = 85	D = 35–44 mm T12Axyz = 82 g	T12Axyz = 82 g	TTI = 85 Shoulder Belt Tension = 1750 lb
Abdomen	Abd F = 562 lb	NA	NA	NA	Abd F = 540 - 630 lb (Total)	NA	No Belt Contact
Pelvis	Pubic F = 1349 lb	NA	NA	Ay = 130 g	Pubic F = 1349 lb	Iliac+acet F = 1147 lb	Ay = 130 g
Lower Limbs	NA	Femur Fz = 2250 lb	Femur Fz = 1530 lb	NA	NA	NA	NA

and assess the potential for injury mitigation provided by inflatable restraint systems. The following specific tasks were accomplished:

- Conducted dynamic tests with typical aircraft side-facing seat configurations using the ES-2 ATD
- Evaluated the potential for injury using current, proposed, and preliminary injury criteria
- Evaluated the ES-2 ATD's functionality when used in the aviation environment
- Investigated test methods unique to side-facing seats
- Evaluated the ability of inflatable restraint systems to mitigate injuries in these seating configurations

RESEARCH PROTOCOL

Industry Survey

An informal survey was conducted to determine the seat geometry and restraint configurations of seats currently being built to meet 14 CFR 23.562, 14 CFR 25.562, and existing FAA policy. Three seat manufacturers provided input. The survey results are summarized in Figures 1 and 2 and Tables 2 and 3. The survey indicates that a restraint geometry with the forward lap and shoulder belt anchor points near the centerline of the occupant (commonly referred to as the body-centered location) has been widely adopted.

Seat Specification

The results of the survey were used to derive a research seat configuration. The specifications of the test seat are identified as the CAMI Configuration in Figure 1 and Table 2. To allow multiple tests to be conducted with a maximum amount of repeatability, a seat with rigid seating support surfaces and rigid belt anchor points was used for the study. Since many side-facing seats are attached to the aircraft side wall in addition to the floor, their seating surfaces and restraint attachment points are typically very stiff. For this reason, use of a rigid seat for this test series should produce similar results to stiffer seat designs and conservative (higher) loading results compared with more flexible seats.

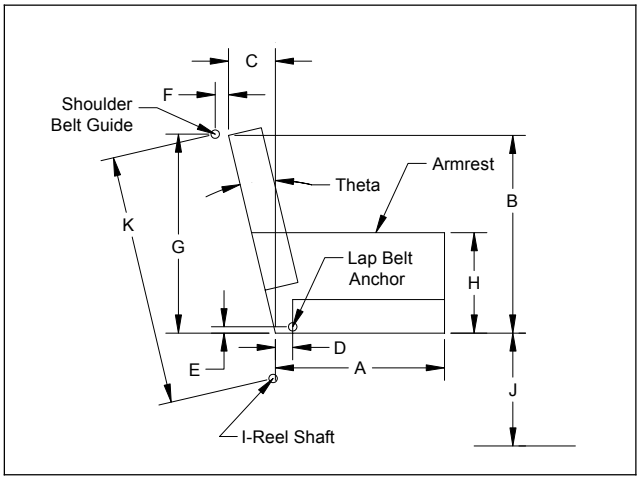

Figure 1 - Seat End View

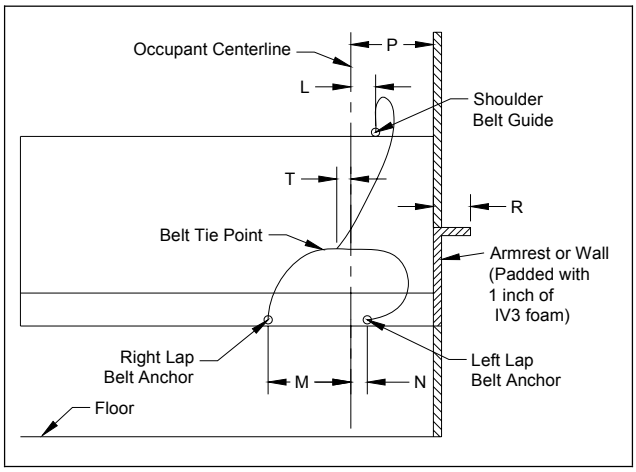

Figure 2 - Seat Front View

Table 2 - Seat Dimensions and Test Configurations Corresponding to Seat End View (Figure 1)

(Dimensions in inches)	A	B	C	D	E	F	G	H	J	K
Manufacturer A	19.3	26.7	3.2	3.4	1.0	1.6	25.7	-	13.3	-
Manufacturer B	20 - 26	18.8	2.2	2.2	0.6	2.9	27.5	-	13.5	-
Manufacturer C	20 - 22	17.4	3.4	2.5	1.0	3.6	24.0	12.0	13 - 14	-
CAMI Configuration	20.2	23.8	5.5	2.1	0.8	1.6	24.1	12.1	13.2	30.0

The seat cushion thickness and the density and stiffness of the foam selected were at the median range of the seat designs surveyed. The foam selected was a DAX 47 that had a density of 3.0 lb/cu ft and a stiffness of 96 - 115 ILD at 65% indention. The cushions were rectangular in shape and covered in upholstery grade, smooth leather. The bottom cushion was 4 in thick by 18 in wide by 22.75 in long. The back cushion was the same thickness and length but was 19 in wide. The cushions were attached to the seat with hook-and-loop fastener material to preclude sliding. The cushions assemblies were supplied by one of the seat manufacturers that participated in the survey.

ATD

The ATD used to assess injury was an ES-2, build level E2.AI. This version differs somewhat from the ES-2re currently proposed for use in the NPRM in that it does not have rib extensions. The primary purpose of the rib extension (re) modification to the ES-2 is to prevent unrealistic interaction between heavily contoured seat cushions, found in typical automobile applications, and the back plate of the ATD when subjected to oblique acceleration vectors (6). Since aircraft side-facing couches are not typically contoured and the tests would be conduced with no yaw, it was determined that the E2.AI version of the ES-2 ATD should provide sufficiently equivalent results for this test series.

An FAA Hybrid-III (7) was also used in one test to allow direct comparison with the ES-2 results and with other side-facing research conducted using the Hybrid-III.

Restraints

Two configurations of restraints were evaluated.

Conventional Restraint. The first restraint was a conventional AMSAFE three-point system consisting of a lap belt and shoulder belt with an inertial reel. A push-button (automotive style) buckle was located on the right side, positioned just above the right thigh. The shoulder belt was attached to the buckle mating tang. The left lap belt segment incorporated a manual length adjustment mechanism. The inertia reel was set to lock at 1.25 G ± .25 G of webbing acceleration.

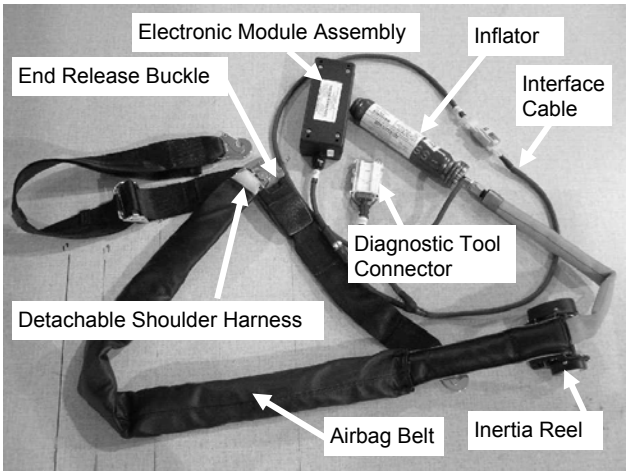

Figure 3 - AAIR System

Inflatable Restraint. The second system evaluated was identical to the first but incorporated an inflatable shoulder belt. The AMSAFE Aviation Inflatable Restraint (AAIR) was designed to function as follows. When exposed to a 16 G horizontal deceleration with a 90 ms linear rise time, the system crash sensor closes the inflation firing circuit at approximately 42 ms. This sends sufficient energy to fire the pyrotechnic initiator in the inflator assembly, releasing stored gas to inflate the tubular restraint. The inflating airbag pretensions the webbing and pre-loads the occupant. After airbag deployment, the restraint deflates to facilitate the occupant's egress from the aircraft with minimal obstruction from the airbag.

Table 3 - Seat Dimensions and Test Configurations Corresponding to Seat Front View (Figure 2)

(Dimensions in inches)	L	M	N	P	R	T	Theta (degrees)
Manufacturer A	0	9.0	0	9.5	-	-	8.0
Manufacturer B	0	13.2	13.2	13.2	-	-	7.0
Manufacturer C	3 - 4	11.3 – 13.3	0	11.3 – 13.3	-	-	11.0
CAMI Center	3.0	10.0	0	40.0	4.5	1.7	13.0
CAMI Close Wall	3.0	10.0	0	10.0	4.5	1.7	13.0
CAMI Far Wall	3.0	10.0	0	13.0	4.5	1.7	13.0
CAMI Armrest	3.0	10.0	0.0	10.0	4.5	1.7	13.0

The crash sensor's predetermined deployment threshold is designed to prevent inadvertent deployment during normal operations, such as hard landings, vibration, or turbulence. The system is activated by joining (buckling) the three-point restraint in the same manner as any other three-point seatbelt. Unbuckling the seatbelt safes the AAIR system.

- The AAIR system consists of these components, illustrated in Figure 3.
- Seatbelt Airbag Assembly (SAA)
- Inflator Assembly
- Electronics Module Assembly (EMA)
- Cable Interface Assembly

The SAA consists of two primary subassemblies: the Three-Point Airbag Belt Assembly and the End-Release Buckle Assembly. The SAA mounts to the aircraft structure using existing mounting points. The End-Release Buckle Assembly provides electrical connection to the Inflator Assembly and the Cable Interface Assembly. The Inflator Assembly mounts under the occupant seat. The Cable Interface Assembly connects the EMA to the SAA and also provides a Diagnostic Tool Connector leg, which allows connection of the System Diagnostic Tool to facilitate system functional checks. The EMA contains the crash sensor electronics and system power (Lithium-type battery) and is mounted to aircraft structure (simulated by the sled floor in this test series).

Test Configurations

Three seat configurations were investigated that represented typical aircraft side-facing seat scenarios. One configuration placed the occupant in the second place of a multiple place couch. The seat position just forward of the occupant was unoccupied. The second configuration placed the occupant adjacent to a rigid wall that was padded with 1 in of IV3 energy-absorbing padding, as called for by AC 25-785 to provide an impact surface typical of an aircraft interior. The padding's secondary purpose was to prevent needless damage to the ATD from impacts with a completely rigid surface. The wall extended beyond the front of the seat sufficiently to support the ATD's lower legs. As part of the second configuration, two occupant/wall distances were investigated. A "Close Wall" configuration positioned the ATD centerline (CL) 10 in from the wall, which corresponded to a 20 in seat width (the narrowest reported in the survey). A "Far Wall" configuration positioned the ATD CL 13 in from the wall, which corresponded to a 26-in seat width (the widest seat reported in the survey). The third configuration placed the occupant adjacent to an armrest with no impact surfaces forward of the armrest and no lower leg support. The ATD CL was 10 in from the armrest. The armrest top and vertical surfaces were padded with 1 in of IV3 padding. Figure 2 and Table 3 provide the pertinent dimensions of each configuration: Center, Close Wall, Far Wall, and Armrest.

Test Conditions

The 16 G, 44 feet per second impact condition defined in 14 CFR 25.562 was used. To limit study variables, no yaw component of deceleration was included. Figure 4 illustrates a typical deceleration pulse for this project.

ATD Placement

Procedures were developed to seat the ATD consistently, with the goal of reproducing the seated position of a 50% male-size human occupant. As the ATD was lowered into the seat, a force of 50 lb was applied horizontally to the knees to compress the back cushion. The lap belt was tightened per the SAE AS8049 procedure that calls for the belt to be tightened until only two fingers can be placed between the belt and the ATD pelvis. The ATD upper torso was then pushed backwards with a nominal amount of force to bring it upright and then tied in place with 32 lb (total) breaking force string. The design of the ES-2 neck permits a significant amount of free head rotation about the Z axis. To align the head and torso midsagittal planes, the head was set at the midpoint of the available range of rotation. The pre-test location of the ATD with respect to the seat was measured for each test. This procedure resulted in a very consistent pelvis location (± 0.1 inch in X and ± 0.3 inch in Y) and a somewhat consistent head CG location (± 0.2 inch in X and ± 1.0 inch in Y). When this same procedure was used with the FAA Hybrid-III, it resulted in a more reclined posture, with the head CG 1.9 in further back than achieved with the ES-2. This difference is primarily due to the protruding, anthropometrically incorrect back plate of the ES-2.

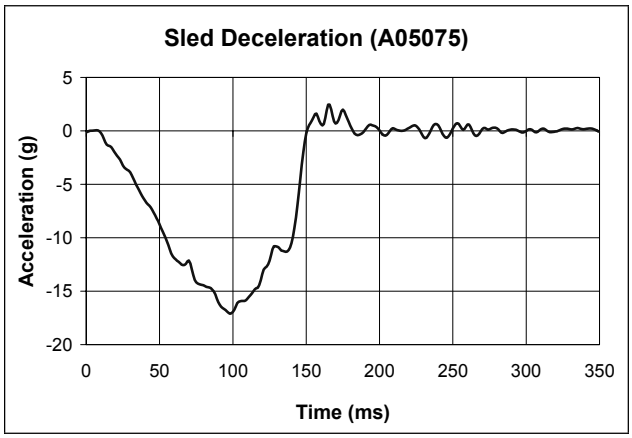

Figure 4 - Typical Sled Deceleration Pulse

Table 4 - ATD Instrumentation

Test Application	Ch. Num	Description	Filter Class	Range	Units
All	3	Head X0 Accelerometer	1000	100	G
All	4	Head X2 Accelerometer	1000	100	G
All	5	Head X3 Accelerometer	1000	100	G
All	6	Head Y0 Accelerometer	1000	100	G
All	7	Head Y1 Accelerometer	1000	100	G
All	8	Head Y3 Accelerometer	1000	100	G
All	9	Head Z0 Accelerometer	1000	100	G
All	10	Head Z1 Accelerometer	1000	100	G
All	11	Head Z2 Accelerometer	1000	100	G
All ES-2	12	T1 X Accelerometer	180	2000	G
All ES-2	13	T1 Y Accelerometer	180	2000	G
All ES-2	14	T1 Z Accelerometer	180	2000	G
All ES-2	15	T12 Y Accelerometer	600	2000	G
All	16	Pelvis Y Accelerometer	600	2000	G
All	17	Upper Neck Fx	600	2250	lb
All	18	Upper Neck Fy	600	2250	lb
All	19	Upper Neck Fz	600	3375	lb
All	20	Upper Neck Mx	600	2655	in-lb
All	21	Upper Neck My	600	2655	in-lb
All	22	Upper Neck Mz	600	2655	in-lb
All	23	Lower Neck Fx	600	2700	lb
All	24	Lower Neck Fy	600	2700	lb
All	25	Lower Neck Fz	600	3150	lb
All	26	Lower Neck Mx	600	3980	in-lb
All	27	Lower Neck My	600	3980	in-lb
All	28	Lower Neck Mz	600	2655	in-lb
All ES-2	29	Upper Rib Deflection	180	3	in
All ES-2	30	Middle Rib Deflection	180	3	in
All ES-2	31	Lower Rib Deflection	180	3	in
All ES-2	32	Upper Rib Y Accelerometer	180	2000	G
All ES-2	33	Middle Rib Y Accelerometer	180	2000	G
All ES-2	34	Lower Rib Y Accelerometer	180	2000	G
All ES-2	35	Pubic Fy	600	4500	lb
All ES-2	36	Torso Back Fy	600	1100	lb
All ES-2	41	Front Abdominal Fy	600	1100	lb
All ES-2	42	Mid Abdominal Fy	600	1100	lb
All ES-2	43	Back Abdominal Fy	600	1100	lb
A05076, A06004	48	Femur Mz	600	3000	in-lb
A06004 (H-III)	12	Chest X Accelerometer	180	200	G
A06004 (H-III)	13	Chest Y Accelerometer	180	200	G
A06004 (H-III)	14	Chest Z Accelerometer	180	200	G
A06004 (H-III)	15	Pelvis X Accelerometer	180	200	G
A06004 (H-III)	29	Pelvis Z Accelerometer	180	200	G

Instrumentation

Electronic Instrumentation. ATDs were instrumented as shown in Table 4. T12 resultant acceleration is referenced in the proposed changes to FMVSS No. 214 (5), but due to channel quantity limitations, only the lateral component of T12 acceleration was recorded for this test series. Since the lateral component should be the largest contributor to the resultant, the lateral component was used to derive the injury criteria for this test series. The tension in the lower segment of the shoulder belt was measured between the inertia reel and the webbing guide for all tests. The tension in the upper segment of the shoulder belt was measured between the belt guide and the shoulder of the ATD for those tests that did not incorporate an inflatable restraint. The tension force in the inflatable segment was estimated by adding the expected frictional losses to the tension measured below the webbing guide. These frictional losses were quantified using data from similar tests that have loads measured on both sides of the webbing guide. The forces exerted on the lap belt attachments were measured for most tests. Due to data channel quantity limitations, the left (more lightly loaded) belt anchor forces were not recorded on some tests. The forces applied to the armrest by the ATD were also measured.

Video Coverage. High-speed (1000 frames per second), high resolution (1024 x 512 pixels) color video was captured from the side and overhead directions by cameras aimed perpendicular to the sled travel. Rectilinear targets were placed on the ATD's forehead, chin, and knees to facilitate motion analysis.

Belt Impingent Detector. A means of determining the areas of the ATD that received significant loading by the shoulder belt was investigated. A 0.5-in thick piece of soft closed cell foam was wrapped around the right side of the ATD's neck and secured with tape. A packing material commonly referred to as "bubble wrap" was taped to the top of this foam layer and directly to the top of the ATD's standard shoulder foam insert. As shown in Figure 5, the specific areas loaded by the belt were indicated by a pattern of burst cells (manually marked with blue dots post-test). The material had 0.45-in diameter cells, distributed in a pattern with 0.1 cells per square in. The measured force required to burst each cell varied from 11 lb to 42 lb. The average burst pressure was 84 psi.

Inertia reel pay out. A piece of string was attached to the shoulder belt and then passed through a block of dense foam fixed to the seat near the inertia reel. By measuring the amount of string pulled though the foam block, the maximum webbing payout during each test was easily determined.

Figure 5 - Belt Impingement Detector

Table 5 - Test Matrix

Configuration	Restraint Type	ATD Type	Test Number
Center	Conventional	ES-2	A05066
		ES-2	A05068
	Inflatable	ES-2	A05067
		ES-2	A05070
Close Wall	Conventional	ES-2	A05065
Far Wall	Conventional	ES-2	A05071
	Inflatable	ES-2	A05072
Armrest	Conventional	ES-2	A05075
		ES-2	A05076
	Inflatable	ES-2	A05073
		ES-2	A05074
	Conventional	FAA H-III	A06004

RESULTS

Test Matrix

Table 5 summarizes by test number the seat configurations, restraint systems, and ATDs evaluated in this test series.

Data Analysis

Data Processing. The test data were gathered and filtered per the requirements of SAE J211/1 (8). The sign convention of the recorded signals conformed to SAE J1733 (9). Upper neck forces and moments reported were normalized to the occipital condyle location. Lower neck forces and moments were normalized to the base of the neck. In addition, the T12, Pelvis Y, and rib accelerations were all processed using the FIR 100 program, as called for by FMVSS No. 214 (10).

Injury Criteria Calculation. Some injury criteria such as Head Injury Criteria (HIC), Thoracic Trauma Index (TTI), and Viscous Criterion (V*C) are derived from test data using mathematical calculations. Instructions for calculating them can be found in the regulations that cite the criteria and in a useful summary report published by the Data Processing Vehicle Safety Workgroup (11).

The HIC was calculated in two ways: HIC after initial contact (as called for by aviation regulations) and HIC15 (as called for in automotive regulations). HIC after initial contact only evaluates impacts that involve head contact and limits the evaluation period to the time of initial head contact until the end of the test. HIC15 is evaluated for the entire test period, regardless of contact, but limits the duration of the HIC interval to 15 ms or less.

The TTI, acceleration-based criteria defined in FMVSS No. 214, was calculated using T12 and rib accelerations that are filtered with the FIR 100 algorithm.

The V*C, deflection-based criteria, was derived from the rib deflection measurements per EU 96/27/EC (12).

Neck Injury Assessment. To limit the potential for neck injury in forward auto crashes, FMVSS No. 208 (13) defines the criteria for neck tension and compression, as well as criteria that combine the effect of neck bending-moment and tension, called Nij. Since the biomechanical basis for the fore/aft Nij criteria may also be applicable to the lateral direction, a preliminary lateral neck injury criteria were developed to allow comparison of tests using the same concept. Soltis et al. suggested intercept values for this preliminary formulation that were derived from existing literature (14). While the tension and compression intercepts suggested are the same as the FMVSS No. 208 values, the lateral bending moment intercepts are much lower and are likely conservative. The formula and intercept values used to calculate the Preliminary Lateral Nij are:

$$N_{ij} = \frac{F_z}{F_{zc}} + \frac{M_{OCx}}{M_{xc}}$$

Fzc (compression) = 1385 lb
Fzc (tension) = 1530 lb
Mxc (right flexion) = 530 in-lb
Mxc (left flexion) = 530 in-lb

The Preliminary Lateral Nij criteria calculated using these suggested intercept values should only be used for comparison between test configurations and not considered as an absolute pass/fail evaluation.

Photometric Analysis. The motions of various ATD body segments were determined from the videos using a 2-D planar photometric technique meeting the requirements of SAE J211/2 and SAE ARP 5482 (15, 16). The excursions reported were essentially a projection of the ATD's three-dimensional motion into a vertical plane parallel to sled travel. While the ATD's head exhibited significant out of plane motion (a maximum of 16 in), the potential perspective error was mitigated (less than 3% understatement) by the 46-ft distance from the sled to the camera. The angle of the head with respect to the vertical was calculated from the measured location of the forehead and chin targets. The maximum angle of the T1 (upper thoracic) vertebrae with respect to the vertical was determined by calculating the angle from the ATD's centerline at waist height to the base of the neck. This calculation should be considered only an estimate since there were no discrete target markers at the desired locations. The maximum angle of the head with respect to T1 was calculated by subtracting the estimated T1 angle from the measured head angle at the corresponding point in time.

Data Summary

Selected measured parameters and calculated injury criteria are summarized in Tables 6 to 8. The results are grouped by similar test configurations. Figure 6 compares the HIC after contact and HIC15 results for the ES-2 tests. The areas of significant shoulder belt contact, as indicated by the investigational Belt Impingement Detector, are summarized in Table 9. Upper and lower neck peak tension, shear, and lateral bending moment responses are summarized in Figures 7 and 8. Shoulder belt forces measured above and below the belt guide are compared in Figure 9. A detailed evaluation of each test configuration and video stills showing the initial condition and point of maximum flail for each test are provided in Appendix A.

Table 6 - Center Configuration

Test parameter	Criteria Limit	Test Number			
		05066	05068	05067	05070
Test Configuration		Center	Center	Center	Center
Restraint		Conv *	Conv *	Inf **	Inf **
Impact Vel (ft/s)		44.6	44.6	44.5	44.6
Impact Acc (g)		-17.4	-17.7	-17.1	-17.4
HIC After Contact	1000	1259	1391	none	none
HIC15	700	1093	1115	103	96
TTI (g)	85	39	39	24	24
V*C (m/s)	1.0	0.0	0.0	0.0	0.0
Pelvis Ay (g)	130	29	28	17	17
Upper Rib Deflection (mm)	35 - 44	0	0	4	2
Middle Rib Deflection (mm)	35 - 44	0	0	4	2
Lower Rib Deflection (mm)	35 - 44	0	0	2	2
T12 Ay (g)	82	35	38	24	24
Front Abdominal Fy (lb)	540-630 Total	15	25	19	18
Mid Abdominal Fy (lb)	540-630 Total	3	5	5	7
Rear Abdominal Fy (lb)	540-630 Total	6	10	35	34
Pubic Fy (lb)	1350	611	712	496	453
T1 Ay (g)		47.1	47.0	25.2	25.1
Nij (Preliminary Lateral)	1.0	1.07	1.05	0.95	0.79
Up Neck Shear Fy (lb)		212	239	74	90
Up Neck Tension Fz (lb)	938	752	729	297	319
Up Neck Moment Mx (in-lb)		-382	-381	402	347
Low Neck Shear Fy (lb)		925	894	-223	-259
Low Neck Tension Fz (lb)		727	760	252	189
Low Neck Moment Mx (in-lb)		3122	2962	860	884
Head Excursion (in)		26.7	26.4	22.3	22.2
Head Latt Angle wrt T1 (deg)		-87	-105	-72	-74
T1 Latteral Angle (deg)		-37	-41	-20	-22
Upper Shldr Belt Tension (lb)	1750	1735	1705	-	-
Lower Shldr Belt Tension (lb)		1113	1094	491	526
Shoulder Belt Payout (in)		1.0	0.8	0.7	1.5
Right Lap Belt Tension (lb)		2882	2971	2285	2385
Left Lap Belt Tension (lb)		959	1043	591	591
Femur Mz (in-lb)		-	-	-	-
Back Plate Fy (lb)		1266	1002	329	322
Arm Rest Fy (lb)		-	-	-	-
Arm Rest Fz (lb)		-	-	-	-

* Conventional Restraint System ** Inflatable Restraint System

Table 7 - Wall Configuration

Test Parameter	Criteria Limit	Test Number		
		05065	05071	05072
Test Configuration		Close Wall	Far Wall	Far Wall
Restraint		Conv	Conv	Inf
Impact Vel (ft/s)		44.0	44.6	44.6
Impact Acc (g)		-16.4	-16.8	-17.0
HIC after contact	1000	537	2014	145
HIC15	700	537	2014	151
TTI (g)	85	22	41	35
V*C (m/s)	1.0	0.1	0.3	0.0
Pelvis Ay (g)	130	21	31	32
Upper Rib Deflection (mm)	35 - 44	28	31	4
Middle Rib Deflection (mm)	35 - 44	19	20	5
Lower Rib Deflection (mm)	35 - 44	14	12	3
T12 Ay (g)	82	22	39	34
Front Abdominal Fy (lb)	540-630 Total	14	21	8
Mid Abdominal Fy (lb)	540-630 Total	25	8	3
Rear Abdominal Fy (lb)	540-630 Total	6	4	35
Pubic Fy (lb)	1350	203	438	323
T1 Ay (g)		24.6	39.5	34.4
Nij (Preliminary Lateral)	1.0	0.35	1.05	1.35
Up Neck Shear Fy (lb)		103	141	49
Up Neck Tension Fz (lb)	938	140	282	290
Up Neck Moment Mx (in-lb)		141	-510	625
Low Neck Shear Fy (lb)		198	371	-299
Low Neck Tension Fz (lb)		112	269	194
Low Neck Moment Mx (in-lb)		889	879	648
Head Excursion (in)		Contact	Contact	Contact
Head Latt Angle wrt T1 (deg)		-36	-7	-62
T1 Latteral Angle (deg)		-4	-11	1
Upper Shldr Belt Tension (lb)	1750	41	348	-
Lower Shldr Belt Tension (lb)		44	228	319
Shoulder Belt Payout (in)		1.0	0.9	1.1
Right Lap Belt Tension (lb)		510	1046	977
Left Lap Belt Tension (lb)		366	668	352
Femur Mz (in-lb)		-	-	-
Back Plate Fy (lb)		159	294	260
Arm Rest Fy (lb)		-	-	-
Arm Rest Fz (lb)		-	-	-

Table 8 - Armrest Configuration

Test Parameter	Criteria Limit	Test Number				
		05075	05076	05073	05074	06004
Test Configuration		Armrest	Armrest	Armrest	Armrest	Armrest (FAA H-III)
Restraint		Conv	Conv	Inf	Inf	Conv
Impact Vel (ft/s)		45.1	45.1	45.1	45.0	45.2
Impact Acc (g)		-17.1	-16.5	-17.4	-17.4	-17.3
HIC after contact	1000	294	298	None	None	None
HIC15	700	735	614	84	79	157
TTI (g)	85	38	39	25	26	-
V*C (m/s)	1.0	0.0	0.0	0.0	0.0	-
Pelvis Ay (g)	130	26	24	24	22	28
Upper Rib Deflection (mm)	35 - 44	0	1	0	1	-
Middle Rib Deflection (mm)	35 - 44	0	1	1	2	-
Lower Rib Deflection (mm)	35 - 44	4	4	3	3	-
T12 Ay (g)	82	32	34	27	27	-
Front Abdominal Fy (lb)	540-630 Total	101	94	52	60	-
Mid Abdominal Fy (lb)	540-630 Total	132	122	28	33	-
Rear Abdominal Fy (lb)	540-630 Total	95	99	37	38	-
Pubic Fy (lb)	1350	398	424	342	374	-
T1 Ay (g)		48.3	48.9	24.7	25.4	-
Nij (Preliminary Lateral)	1.0	1.47	1.50	0.92	0.87	1.17
Up Neck Shear Fy (lb)		207	198	73	70	214
Up Neck Tension Fz (lb)	938	789	735	289	271	430
Up Neck Moment Mx (in-lb)		668	681	414	394	595
Low Neck Shear Fy (lb)		673	648	-242	-246	304
Low Neck Tension Fz (lb)		780	713	223	232	451
Low Neck Moment Mx (in-lb)		2458	2394	698	684	2022
Head Excursion (in)		25.0	24.9	18.4	18.2	22.7
Head Latt Angle wrt T1 (deg)		-122	-132	-59	-58	-74
T1 Latteral Angle (deg)		-46	-45	-19	-18	-35
Upper Shldr Belt Tension (lb)	1750	1529	1458	-	-	813
Lower Shldr Belt Tension (lb)		995	948	410	418	471
Shoulder Belt Payout (in)		0.9	0.8	1.0	0.7	0.7
Right Lap Belt Tension (lb)		1401	1419	1166	1150	1056
Left Lap Belt Tension (lb)		-	-	-	-	525
Femur Mz (in-lb)		-	1167	-	-	1298
Back Plate Fy (lb)		723	637	306	359	-
Arm Rest Fy (lb)		2726	2715	2290	-	2993
Arm Rest Fz (lb)		848	820	502	526	1050

Table 9 - Belt Impingement Detector Results

Configuration	Restraint Type	Test Number	Number of Burst Cells In Each Area	
			Shoulder	Base of Neck
Center	Conv	A05066	0	1
Center	Conv	A05068	4	3
Center	Inf	A05067	0	1
Center	Inf	A05070	1	0
Close Wall	Conv	A05065	0	0
Far Wall	Conv	A05071	0	1
Far Wall	Inf	A05072	0	3
Armrest	Conv	A05075	7	0
Armrest	Conv	A05076	6	0
Armrest	Inf	A05073	1	1
Armrest	Inf	A05074	2	8
Armrest (FAA H-III)	Conv	A06004	6	7

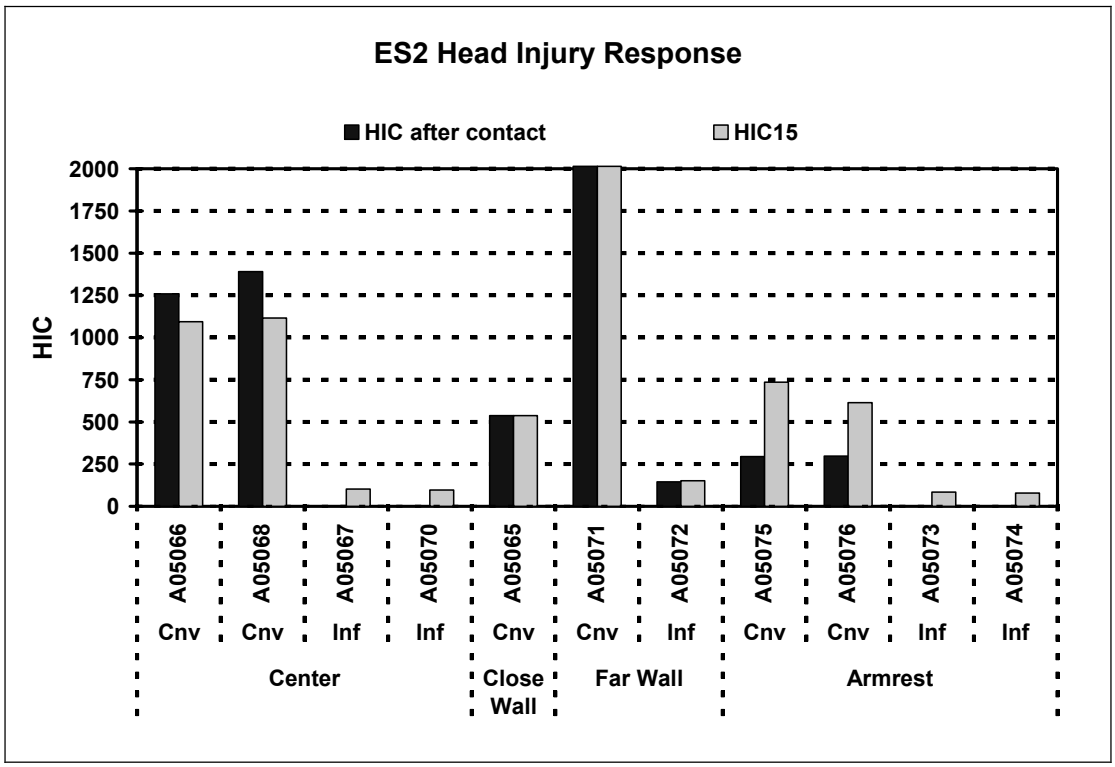

Figure 6 – ES-2 Head Injury Response

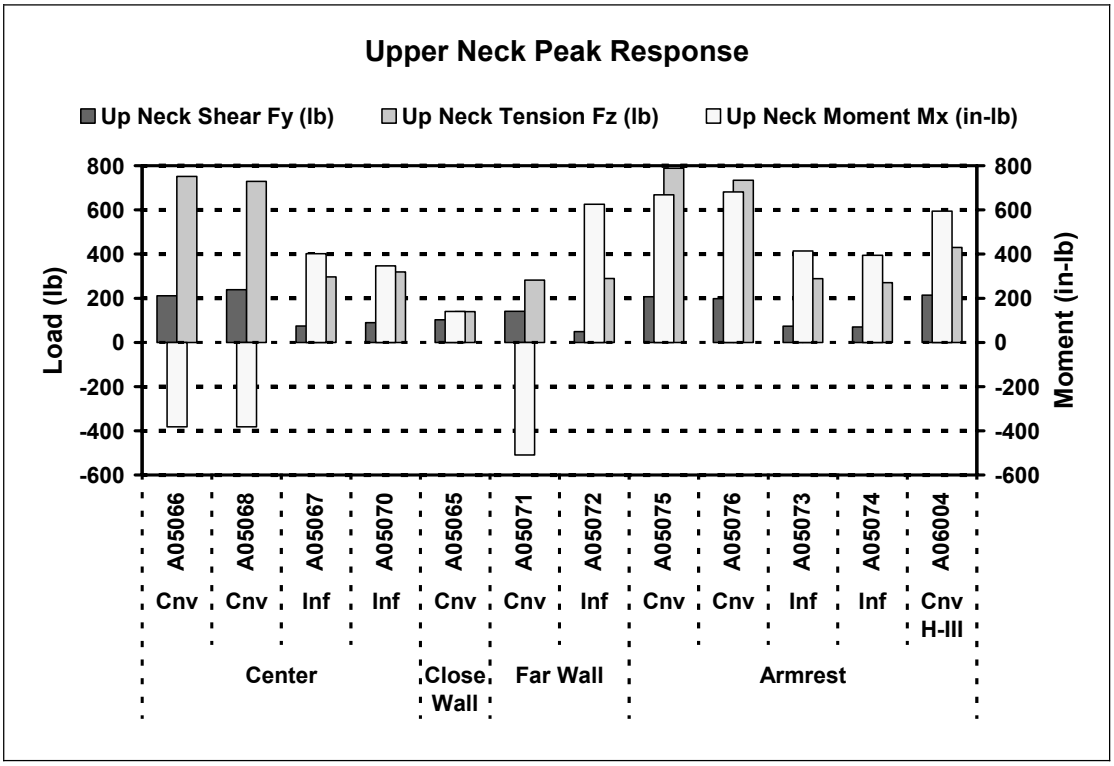

Figure 7 – Upper Neck Peak Response

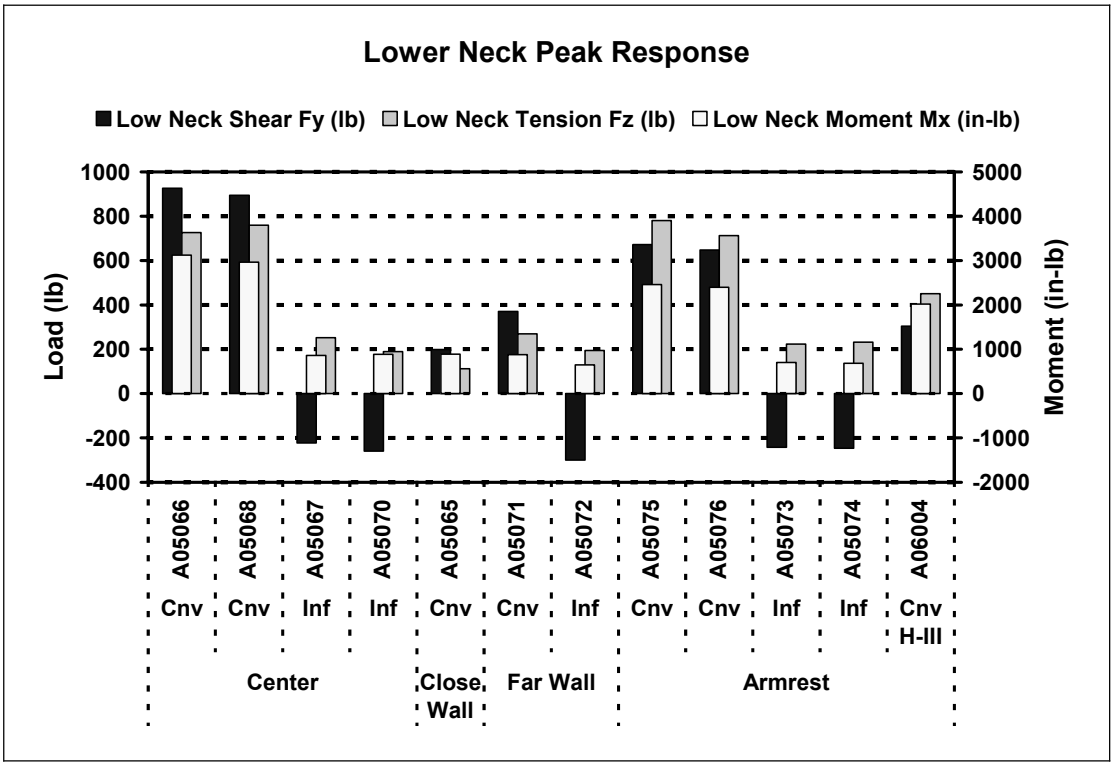

Figure 8 – Lower Neck Peak Response

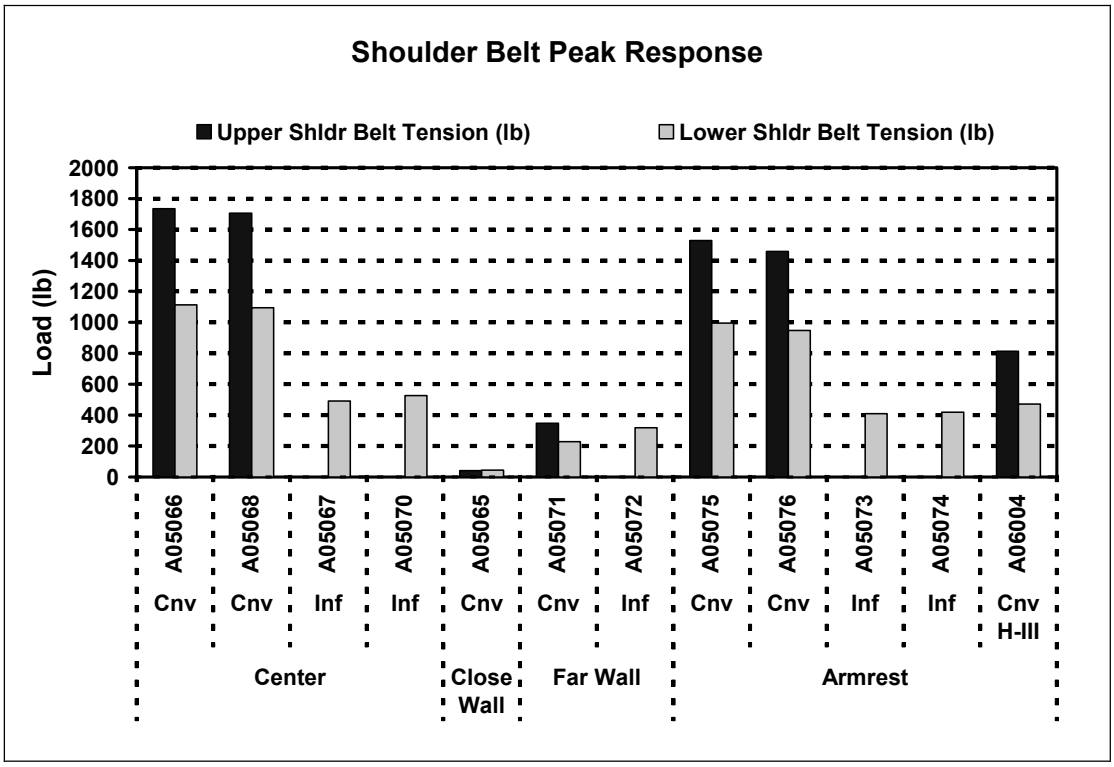

Figure 9 – Shoulder Belt Peak Response

Table 10 - Summary for Each Seat Configuration Tested, the Body Regions at Greatest Risk for Injury, and the Injury Criteria Indicating the Risk

Body Region	Tested Seat Configurations (Conventional Restraint)			
	Center	Close Wall	Far Wall	Armrest
Head	HIC		HIC	HIC15
Neck	Nij Prelim		Nij Prelim	Nij Prelim
Thorax	Belt Tension		Rib Def	Belt Tension
Abdomen				
Pelvis				
Leg				Femur Mz

CONCLUSIONS

Injury Assessment

Table 10 summarizes for each seat configuration tested the body regions at greatest risk for injury and the injury criteria indicating the risk.

For the Center and Far Wall seat configurations, the calculated HIC values indicate that head injury is a significant risk. The lateral flail envelope of the conventionally restrained occupants allowed head contact with adjacent walls and seat structure. For the Armrest configuration, the head did not contact any injurious objects; however, the value of HIC15 was at or near its established limit of 700. HIC15 is an automotive injury criterion used to assess the head injury risk for both contact and inertial loading situations.

The injury potential, represented by the lateral neck forces/moments and belt contact forces measured, are not currently well defined. The measured Preliminary Lateral Nij values are well above the limit in the Armrest and Center configurations. In the Armrest configuration, the upper neck tension is within the current FMVSS No. 208 limits, but the upper neck bending moment is well above the AIS-2 injury levels cited by Soltis et al. (10). In these configurations, the maximum lateral neck angle is also well beyond the cited AIS-2 limits. While there is no current regulatory limit, it should be noted that the magnitude of the lower neck tension and shear forces measured during the Center and Armrest tests were also very high. The impingement instrumentation indicated that the shoulder belt contacted the base of the neck during many of the tests. The magnitude of these loads is unknown since the construction of the ATD permitted the belt to apply forces to the ATD structure below the level of the lower-neck load cell.

None of the injury measurements indicated a significant risk of injury to the chest, abdomen, or pelvis for this group of seat configurations. The upper-shoulder belt tension was just below the limit in the Center configuration tests, and the upper-rib deflection approached the lower bound of the proposed limits in the Far Wall configuration test. All of the other injury criteria for these body segments were well below limits. This is likely due to the effectiveness of the body-centered lap belt in controlling lateral motion of the pelvis. This directly limits pelvic injuries and reduces the loads on the abdomen and chest by reducing the effective mass of the torso. This finding does not imply that injuries could not occur with other side-facing seat configurations. Placing the lap belt anchors at their conventional locations beside each hip could increase pelvis accelerations and forces. Inclusion of an armrest in a seat with a conventional restraint configuration could also lead to high abdominal loading. A combination of ineffective pelvic and torso restraints could also increase chest accelerations and deflections during impacts with adjacent walls.

The high femur twisting-moment measured in the Armrest configuration is a unique loading condition for which an injury criteria has not been established. The intent of the femur compression limits in FAA transport aircraft regulations was to avoid injuries that would impede evacuation. In a similar fashion, a limit on the twisting moment may be necessary to provide the intended level of safety.

Test Method Evaluation

Some tests were repeated to assess result variability. In all cases, occupant kinematics and recorded parameters were very similar for the repeated tests. This indicates that the ATD placement procedures developed were effective in achieving consistent results. Further study is needed to develop placement procedures that result in a recline angle more representative of a human occupant.

Inflatable Restraint Evaluation

In most cases, the inflatable restraints were effective in reducing the lateral flailing of the occupant and significantly reduced the head accelerations, neck loads, chest acceleration, rib deflections, and the injury criteria derived from these measurements. In only one case (the Far Wall configuration) were measured parameters significantly greater than without the inflatable. In this case, while the inflated torso restraint reduced the severity of impact with the adjacent wall, it acted as a fulcrum around which the head rotated laterally, increasing the upper-neck bending moment. The inflatable restraints did not limit the lateral flail envelope sufficiently to preclude significant "body to body" contact with an adjacent occupant (if present). Further development was conducted by AMSAFE to determine if it is possible with current technology to prevent "body to body" contact (17). Use of an inflatable restraint similar to the tested systems in conjunction with body-centered lap belt geometry may mitigate many of the injury risks presented by side-facing seat designs that are similar to the test seat configuration.

ATD Evaluation

Overall, the ES-2 functioned well in these types of tests but some issues were noted. Special ATD installation procedures may be required to achieve the proper (human-like) initial position, due to interaction between the ATD's protruding back plate and the seat back. The ES-2 (like most side-facing test dummies) was designed to primarily assess injuries caused by direct contact with adjacent interior structure. The foam on top of the shoulder is very soft, and there is no structure that simulates the

human clavicle. This allows the shoulder belt to penetrate significantly into the top of the shoulder and front of the torso at relatively low loads. This response would not be expected with human occupants who have bony support structures in these areas and certainly would not occur with frontal test dummies that have very stiff structures in these areas. This unrealistic interaction with the top of the shoulder also allows the belt to apply forces to the upper torso below the level of the lower neck load cell, resulting in understated lateral shear force readings. Lack of biofidelity in the ES-2 shoulder may increase the lateral flail envelope, compared to the Hybrid-II or FAA Hybrid-III ATDs. On the other hand, because neither the ES-2, the Hybrid-II, nor the FAA Hybrid-III ATDs have flexibility in the mid-spine, their lateral flail envelope could be less than that of a human occupant of similar size when restrained by belts or armrest structure. The ES-2's neck is very flexible, providing superior biofidelity. Tensile strength of the design is apparently much less than on typical forward-facing ATDs. Accordingly, the ES-2 cannot be lifted by its head as with other test dummies since the repeated loading could damage the neck. Loads encountered during some test scenarios were sufficient to damage the neck's rubber center section. Because of this, a thorough inspection of the neck for damage is necessary after tests that result in high loading. High back plate lateral forces were measured in tests with significant lateral flailing. The mechanism that caused the back plate loads is unknown and requires further investigation.

Recommendations

The ES-2 provides a means of assessing the potential for injury using state-of-the-art understanding of side-facing injury mechanisms. Use of the rib deflection, chest acceleration, abdominal forces, and pelvic force limits contained in the proposed FMVSS No.214, in lieu of the current TTI and pelvis acceleration limits would provide the same safety benefits for occupants of aircraft seats as they would for motorists. Use of the ES-2 also allows assessment of potential aircraft-specific criteria for limits on neck loading, femur torsion, and body-to-body contact. The current limits on HIC and shoulder belt tension cited in the aviation regulations, while not specifically validated for side-facing impacts, remain useful indicators of injury for the head and thorax.

The high neck loads measured in some seat configurations emphasize the need for appropriate lateral neck injury criteria. Improvements in the ES-2 shoulder's biofidelity would allow better assessment of the potential for injury caused by belt contact forces.

This study has demonstrated that the injury criterion contained in the current FAA policy, proposed motor vehicle safety standards, and preliminary neck-injury criteria can be effectively met with a combination of seat design features and advanced restraint systems.

REFERENCES

1. U.S. Code of Federal Regulations, Title 14, Parts 23.562, 25.562, 27.562, 29.562. Washington, DC: US Government Printing Office.
2. Lankarani H, Gowdy RV, DeWeese R, et al. Compliance Criteria for Side Facing Seats. Warrendale, PA: SAE International; Apr. 1999; SAE Report No: 1999-01-1598.
3. Transport Airplane Directorate ANM-100. Policy Statement on Side Facing Seats on Transport Category Airplanes. Washington, DC: Federal Aviation Administration; May 2005; Letter No. ANM-03-115-30.
4. Kuppa, S. Injury Criteria for Side Impact Dummies. Washington, DC: National Highway Traffic Safety Administration; May 2004.
5. U.S. Code of Federal Regulations, Title 49, Parts 571 and 598, Federal Motor Vehicle Safety Standards, Side Impact Protection, Phase-In Reporting Requirements, Proposed Rule. Washington, DC: National Highway Traffic Safety Administration; May 2004; Docket No. NHTSA-2004-17694.
6. Vehicle Research and Testing Center. Design, Development, and Evaluation of the ES-2re Side Crash Test Dummy. Washington, DC: National Highway Traffic Safety Administration; May 2004.
7. Gowdy RV, DeWeese R, Beebe M, Blaker J, et al. A Lumbar Spine Modification to the Hybrid-III ATD for Aircraft Seat Tests. Warrendale, PA: SAE International; Apr. 1999; Report No: SAE 1999-01-1609.
8. SAE International. Instrumentation for Impact Test – Part 1- Electronic Instrumentation. Warrendale, PA: SAE International; Dec 2003; Surface Vehicle Recommended Practice No: J211-1.
9. SAE International. Sign Convention for Vehicle Crash Testing. Warrendale, PA: SAE International; Dec. 1994; SAE Surface Vehicle Information Report No: J1733

10. US Code of Federal Regulations, Title 49, Part 571.214. Washington, DC: US Government Printing Office.

11. Data Processing Vehicle Safety Workgroup. Crash Analysis Criteria Description, Version 1.6.2. The Workgroup; April 2005; accessed from: www.crashnetwork.com (Aug. 2006).

12. European Union Side Impact Directive 96/27/EC. European Union; May 1996.

13. US Code of Federal Regulations, Title 49, Part 571.208. Washington, DC: US Government Printing Office.

14. Soltis S, Frings G, van Hoof J, et al. Development of Side Neck Injury Criteria and Tolerances for Occupants of Sideward Facing Aircraft Seats. NATO/PFP; May 2003; RTO-MP-AVT-097.

15. SAE International. Instrumentation for Impact Test – Part 1- Photographic Instrumentation. Warrendale, PA: SAE International; May 2001; SAE Surface Vehicle Recommended Practice No: J211-2.

16. SAE International. Photometric Data Acquisition Procedures for Impact Test. Warrendale, PA: SAE International; May 2003; SAE Aerospace Recommended Practice No: ARP5482.

17. Green T, Barth T. Injury Evaluation and Comparison of Lateral Impacts When Using Conventional and Inflatable Restraints. Creswell, OR: SAFE Association; Oct. 2006.

18. European Enhanced Vehicle-Safety Committee, Working Group 12. Development and Evaluation of the ES-2 Test Dummy. The Committee; Aug. 2001; accessed from: www.eevc.org (Aug. 2006).

APPENDIX A
Detailed Test Evaluation

CENTER CONFIGURATION TEST OBSERVATIONS

Center Configuration - Conventional Restraint. (Figures A1 to A4)

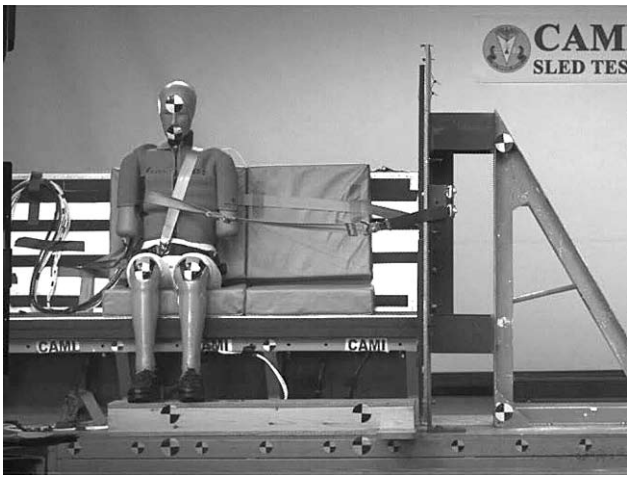

Figure A1 - A05066 T = 0

- The action of the legs flailing forward turns the entire torso about the Z axis of the occupant to partially align it with the deceleration vector.
- The upper-torso restraint did not control lateral flailing well. The 12-in length of belt between occupant's shoulder and shoulder belt guide allows the torso to swing in a combined horizontal and lateral arc that produces a significant head impact with the seat back at the center of the next seat place. The shoulder belt crushed the soft shoulder foam, penetrating 2 in below the nominal shoulder height. Shoulder belt forces were near the limit.
- Upper-neck tension was within 80% of the FMVSS No. 208 limit, and the Preliminary Lateral Nij was 1.05.
- Since there was no lateral contact between the ribs and any structure or restraint system, the rib deflections were negligible, and the rib accelerations were low.
- Lack of lateral contact also limited the magnitude of T1 and T12 accelerations.
- The body-centered lap belt configuration effectively controls lateral excursion of pelvis and the associated lateral acceleration and pubic force.
- High lateral shear forces were measured by the backplate load cell. It is unclear whether this was caused by interaction with the seat cushion or by direct impingement of the shoulder belt during extreme lateral flailing.

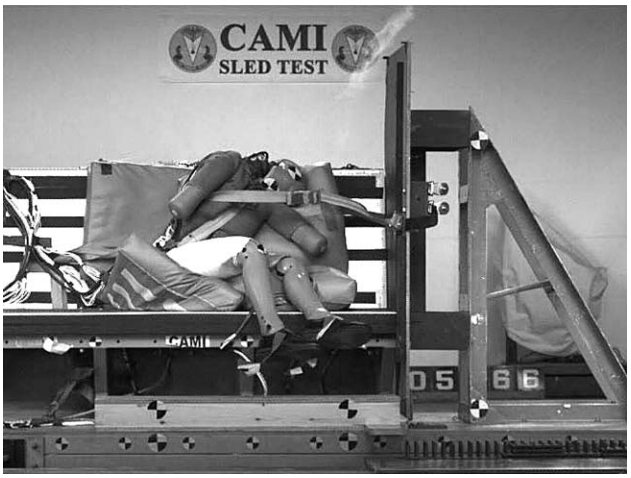

Figure A2 - A05066 T = 151

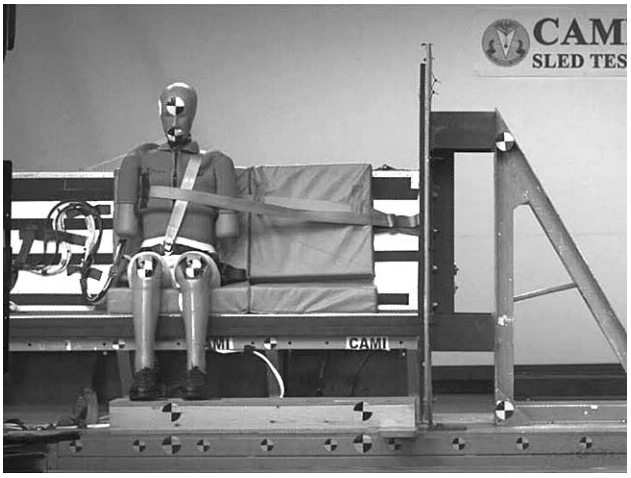

Figure A3 - A05068 T = 0

Figure A4 - A05068 T = 151

Center Configuration - Inflatable Restraint. (Figures A5 to A8)

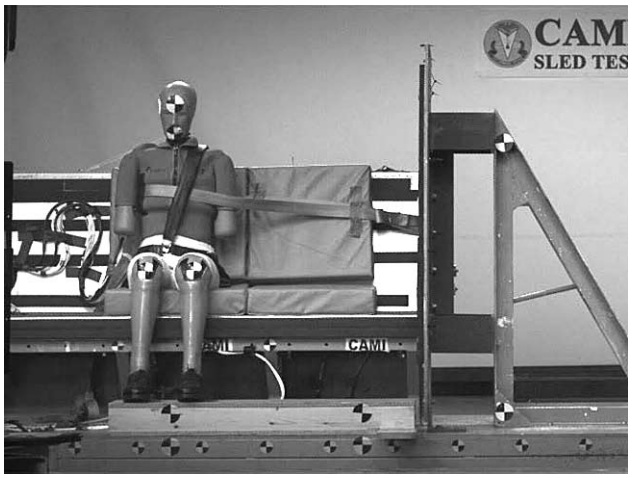

Figure A5 - A05067 T = 0

Figure A6 - A05067 T = 168

- This restraint produced similar kinematics to the conventional restraint except lateral head flailing was significantly reduced.
- The inflatable shoulder belt was fully inflated within 60 ms after impact. The shoulder belt assumed a tube shape that spread the contact forces out over the shoulder, neck, and side of head. The action of filling the inflatable shortens the belt somewhat, which tightens the system and applies a 300 lb preload (measured behind the belt guide). This configuration prevented significant head impact with seat structure.
- Upper-neck tension was reduced significantly. Lower-neck tension and lateral shear forces were both reduced significantly.
- The improvement in upper-torso restraint reduced chest accelerations and shoulder belt forces. Pelvic accelerations and forces, as well as lap belt forces, were also reduced (probably due to the affect of belt pre-tension).
- As with the conventional restraint, the body-centered lap belt configuration effectively controls lateral excursion of pelvis and the associated lateral acceleration and pubic force.

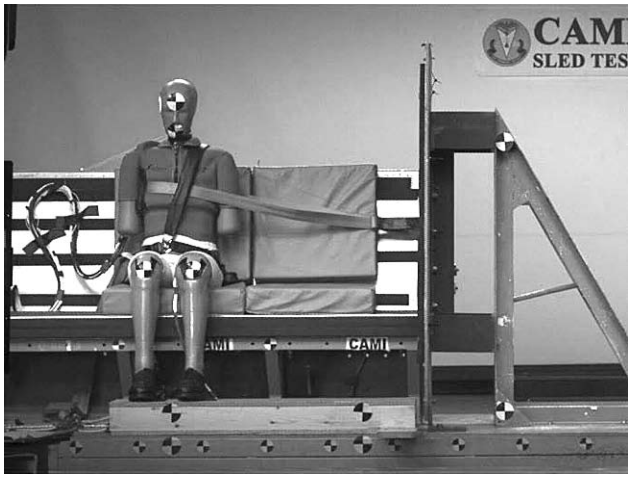

Figure A7 – A05070 T = 0

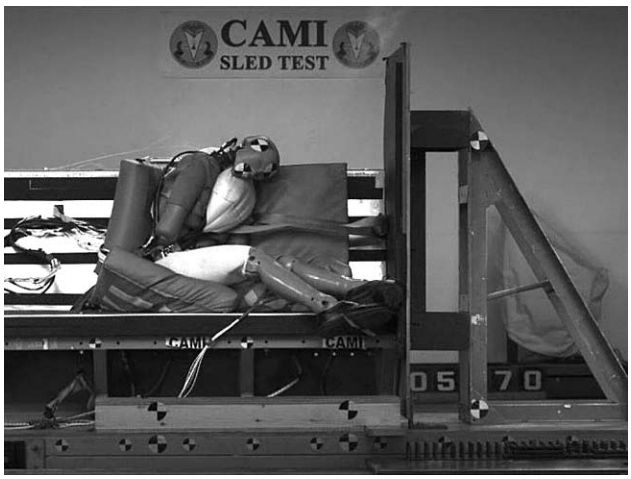

Figure A8 - A05070 T = 168

WALL CONFIGURATION TEST OBSERVATIONS

Wall Configuration - Conventional Restraint. (Figures A9 to A12)

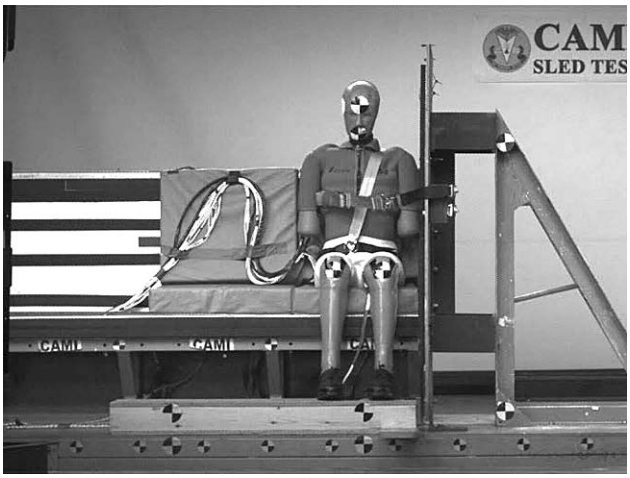

Figure A9 - A05065 T = 0

- Since the legs were supported by the wall, the torso remained side-facing throughout the event.
- The torso restraint was ineffective in preventing head and torso contact with wall surface for either occupant-to-wall spacing. Head impact severity with the wall was low for the close spacing and quite high for the larger spacing.
- The Preliminary Lateral Nij was 1.05 for the Far Wall and occurs as the top of the head impacts the wall, creating a negative moment at the upper neck.
- The ribs contacted the wall surface, producing a moderate level of acceleration and deflections approaching the lower limit for both occupant-to-wall spacings investigated. Figure A13 provides the rib deflection time history for the test that had the maximum deflection measured during this series (upper rib, test A05071). The deflection response did not exhibit the "flat topping" anomaly that can indicate rib-guide binding. Prior studies identified this as a common problem with the EuroSID-1 and led to the development of improved rib guides that were incorporated in the ES-2 (18). T-12 acceleration and TTI were also well within limits.
- The body center lap belt configuration effectively controlled lateral excursion of pelvis to the extent that it prevented significant pelvis contact with the wall for both occupant-to-wall spacings. This resulted in much lower pelvis accelerations and pubic forces than would be expected if contact had occurred.

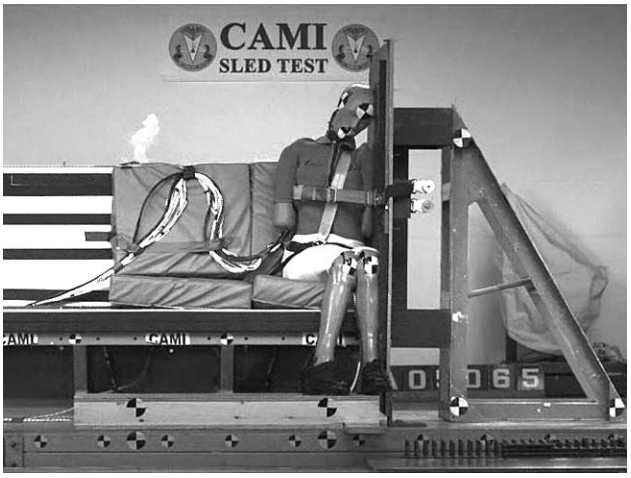

Figure A10 - A05065 T = 101

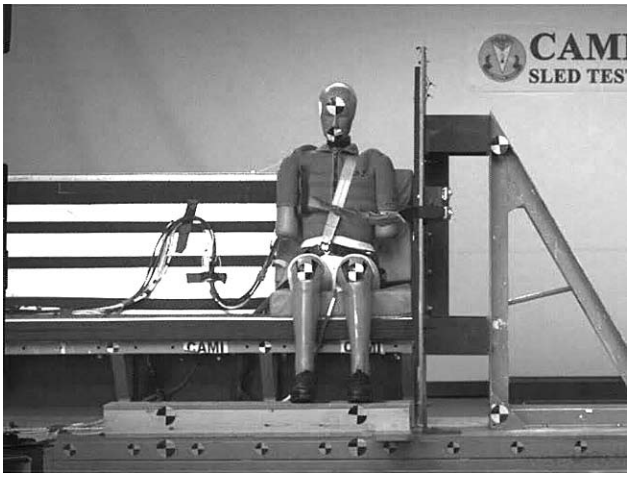

Figure A11 – A05071 T = 0

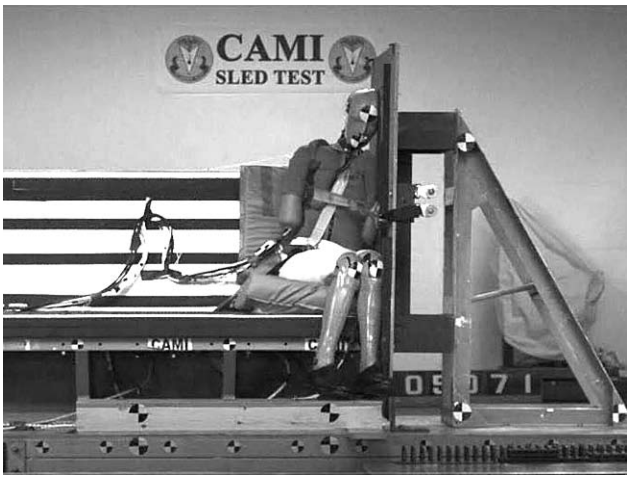

Figure A12 - A05071 T = 106

Wall Configuration - Inflatable Restraint.
(Figures A14 to A15)

- After filling, the inflatable restraint was positioned between the wall and the ATD's head. The kinematics of the lower torso and legs was similar to that produced by the conventional restraint.
- The inflatable restraint acted as a cushion between the head and the wall, significantly reducing the severity of the head contact with the wall.
- Upper-neck lateral bending moments and Preliminary Lateral Nij were higher than with the similar conventional restraint and the other seat configurations with inflatable restraints. In this case, the reaction surface provided by the wall increased the inflatable's effectiveness in reducing the lateral excursion of the neck. This effect apparently raised the point of lateral rotation to the top of the neck as the head rotated laterally over the inflated belt.
- The improved upper-torso restraint resulted in less lateral torso movement and significantly reduced the severity of the contact between the thorax and the wall, nearly eliminating rib deflection.
- Pelvis forces and accelerations were similar to the conventional restraint test.

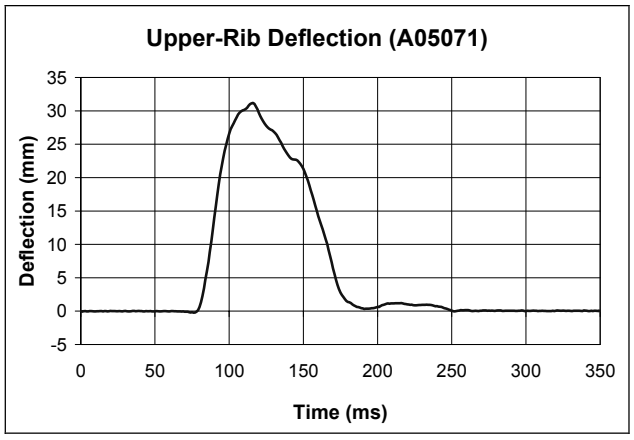

Figure A13 - Maximum Rib Deflection

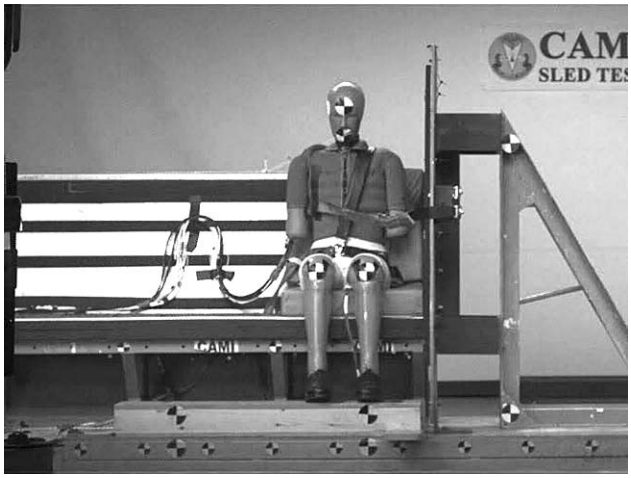

Figure A14 - A05072 T = 0

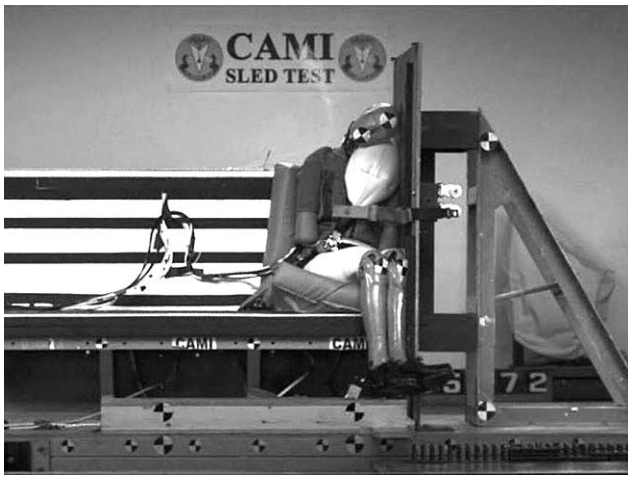

Figure A15 - A05072 T = 122

ARMREST CONFIGURATION TEST OBSERVATIONS

Armrest Configuration - Conventional Restraint. (Figures A16 to A27)

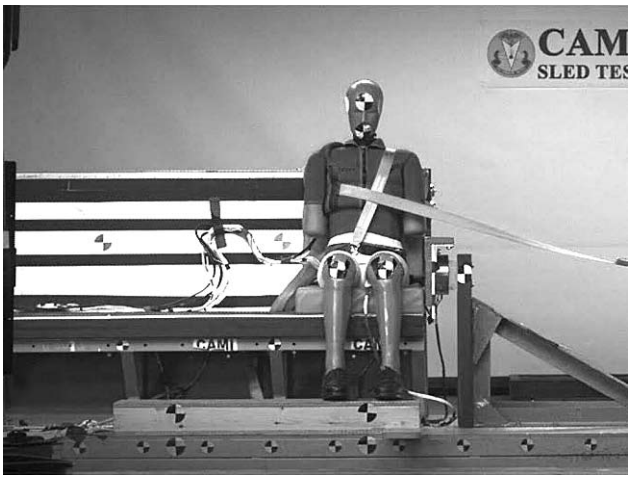

Figure A16 - A05075 T = 0

- The ATD's upper legs were supported by the armrest, keeping the pelvis and torso side-facing during the test.
- The upper-torso restraint did not control lateral flailing well. The 12-in length of belt between occupant's shoulder and shoulder belt guide allowed the torso to swing in a combined horizontal and lateral arc that resulted in head excursion well beyond the armrest and behind the plane of the seat back. The shoulder belt crushed the soft shoulder foam, penetrating 2 in below the nominal shoulder height. The head did not contact any structure but made significant contact with the left shoulder, producing a value of HIC15 that was at or approaching its limit of 700 for both tests.

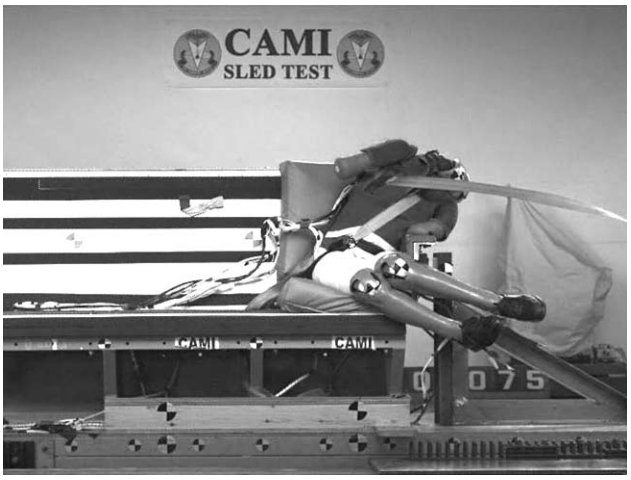

Figure A17 - A05075 T = 168

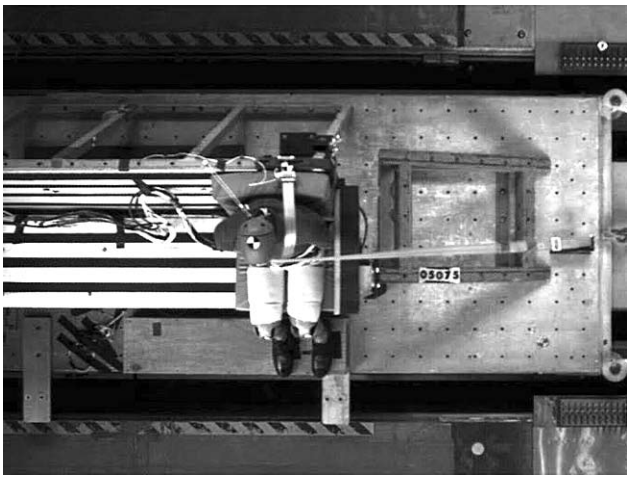

Figure A18 - A05075 (overhead) T = 0

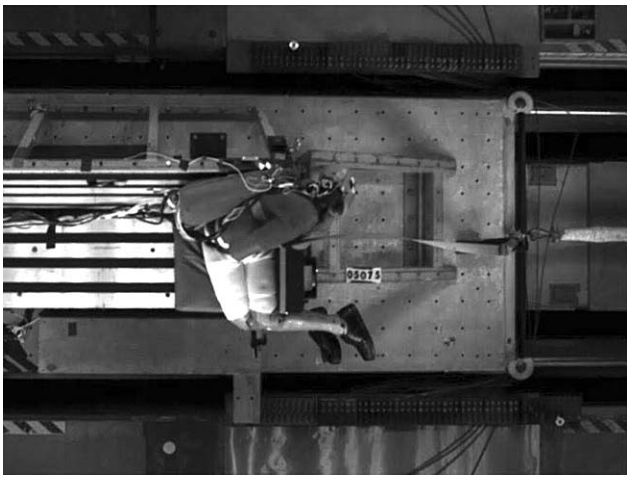

Figure A19 - A05075 (overhead) T = 165

- The "head lag" effect exhibited by human subjects (14) was replicated well by the ES-2 in these tests. This effect produces negative upper neck bending moments due to the inertia of the head during the first phase of a lateral impact. The moments rapidly reverse direction when the head "catches up" to the rotation of the torso. Figure A24 illustrates this effect. In this case, the neck flexed so far that the head contacted the top of the right shoulder. This extreme flailing produced very high upper-neck tension and lateral bending moments, as shown in Figure A25. These forces and moments produced the highest Preliminary Lateral Nij value (1.5) of any configuration tested in this series. Lower-neck tension was also the highest recorded of any of the configurations. It should be noted that after test A05076, a 1.5-in wide separation was found in the middle of the right-front quadrant of the rubber neck. This part failure may have affected the test results. However, since the results were consistent with the immediately preceding test in which this failure had not been noted, it was decided to include the data from A05076 in the comparison.

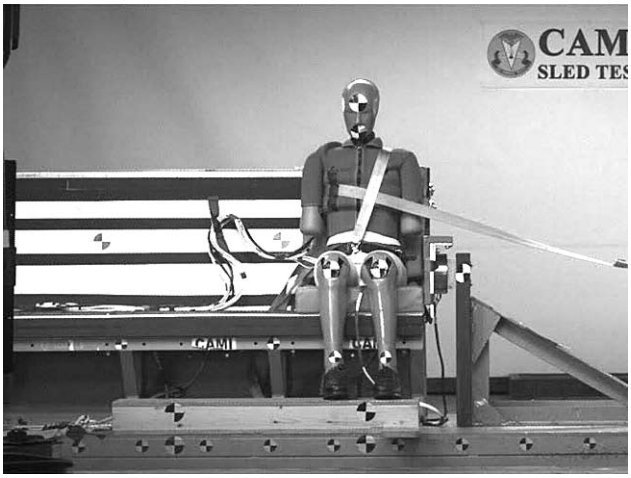

Figure A20 - A05076 T = 0

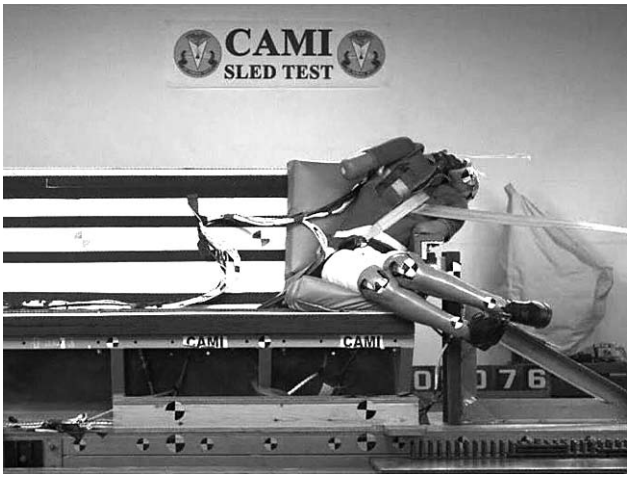

Figure A21 - A05076 T = 168

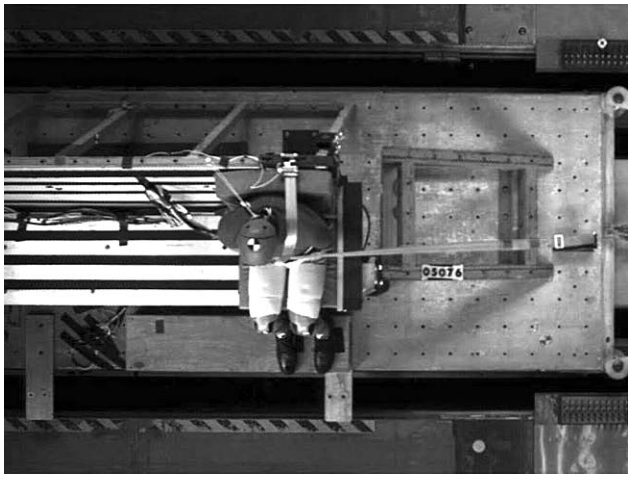

Figure A22 - A05076 (overhead) T = 0

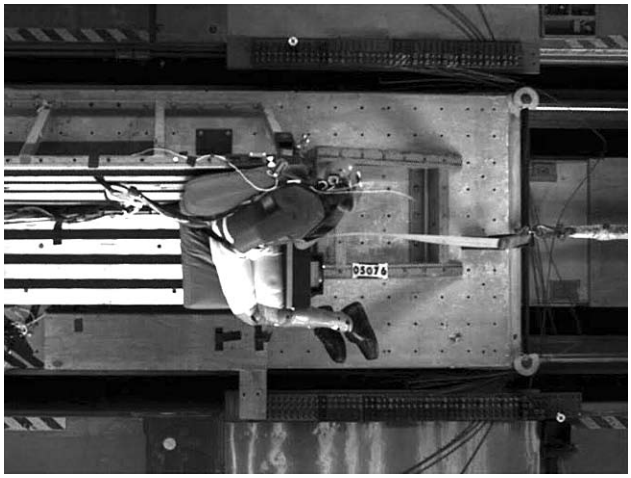

Figure A23 - A05076 (overhead) T = 165

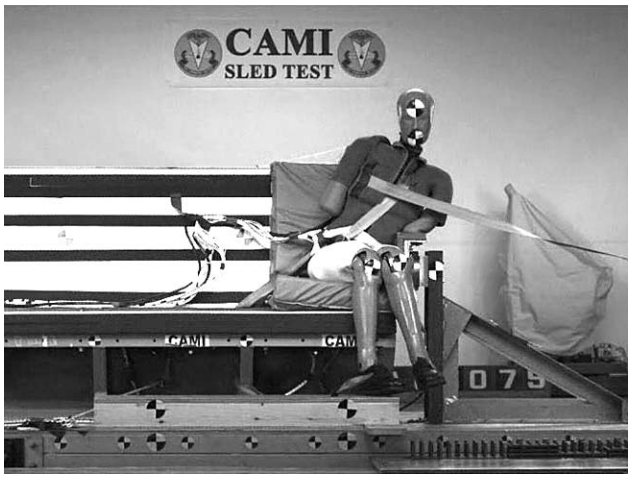

Figure A24 - A05075 T = 110 (Head Lag)

- As the ATD flailed laterally, the left arm became entrapped between the chest and the top of the armrest. This applied some force to the lower rib, compressing it somewhat. Chest accelerations and rib deflections were all far below limits.
- As was observed with the Close Wall configuration, the body-centered lap belt geometry effectively controlled lateral excursion of pelvis to the extent that it prevented significant pelvis contact with the armrest.
- Due to the action of the ATD flailing over the corner of the armrest, abdominal loads were much higher than in the other test configurations. The total load, however, was well below limits.
- The left thigh was supported by the armrest, resulting in both lower legs flailing in an arc that applied a twisting-moment to the femur. Figure A26 shows the lower-leg angle time history for both the ES-2 and the H-III tests. Figure A27 shows the relationship between the femur twisting moment and the lower-leg angle observed during these tests. Essentially, the lower legs of the ES-2 swung freely in an arc about the long axis of the femur until the mechanical stop in the hip joint was reached. At this point, the twisting-moment rose rapidly.
- High lateral shear forces were measured by the backplate load cell. It is unclear whether this was caused by the interaction with the seat cushion or by direct impingement of the shoulder belt during extreme lateral flailing.

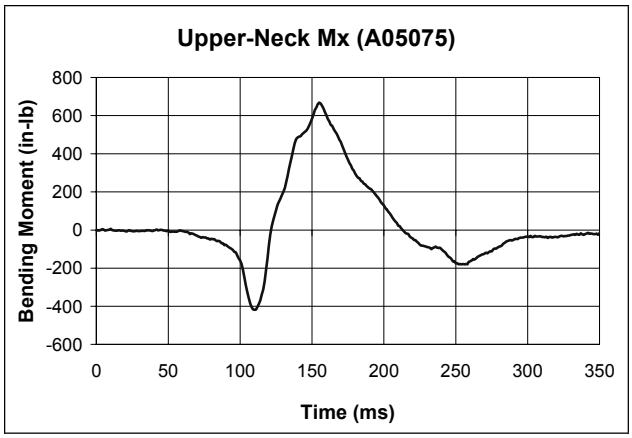

Figure A25 – A05075 Upper Neck Mx

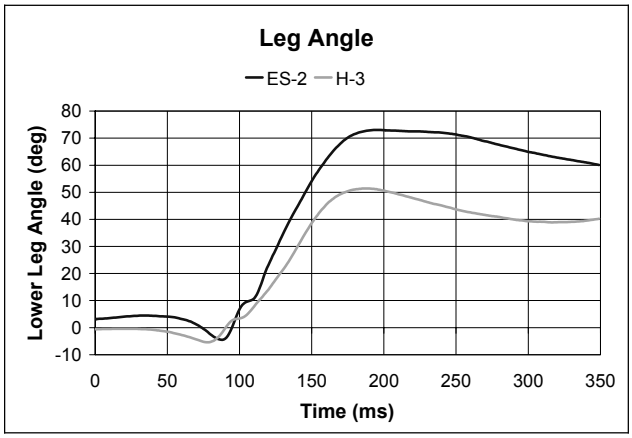

Figure A26 – Lower Leg Angle

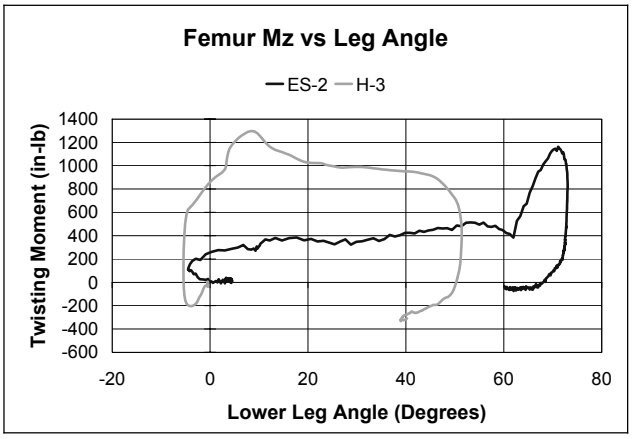

Figure A27 - Femur Twist vs. Lower Leg Angle

Armrest Configuration - Inflatable Restraint.
(Figures A28 to A35)

- As in the conventional restraint test, the torso and pelvis remained side-facing.
- The inflatable restraint improved the upper-torso restraint significantly. The head's forward excursion was reduced considerably (6.7 in less), and the rearward excursion seen in the conventional restraint tests was completely eliminated. Head accelerations were significantly reduced.
- The "head lag" effect was mitigated by the reduced upper torso excursion. Upper- and lower-neck forces and moments were all significantly reduced.

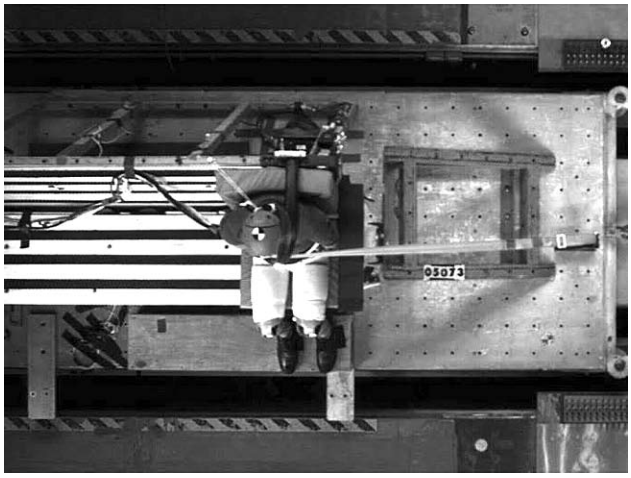

Figure A30 - A05073 (overhead) T = 0

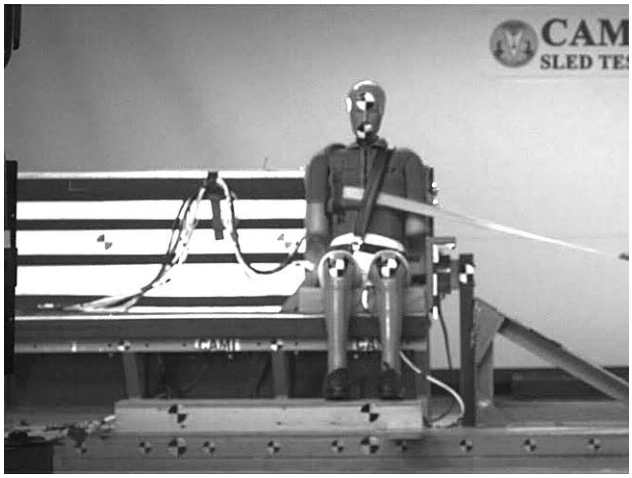

Figure A28 - A05073 T = 0

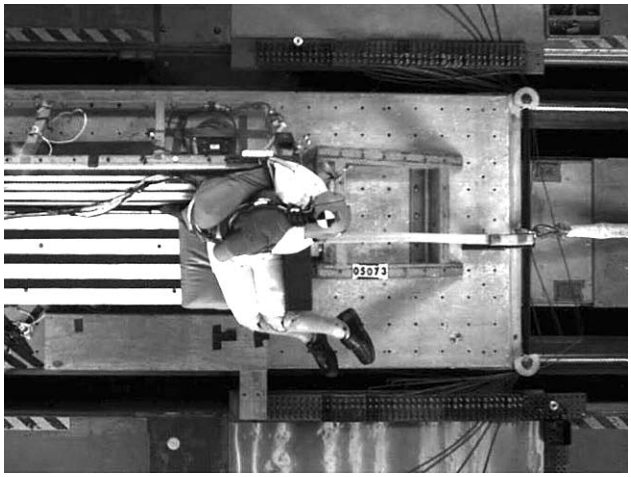

Figure A31 - A05073 (overhead) T = 151

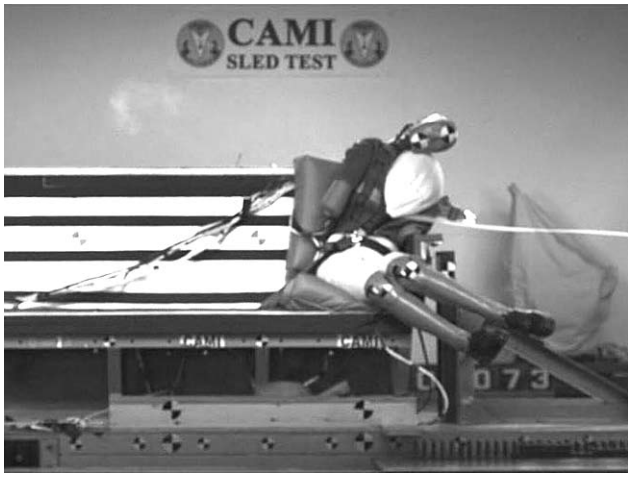

Figure A29 - A05073 T = 158

- The interaction of the ATD arm and the armrest was similar to what was observed with the conventional restraint system. Overall, chest accelerations, rib deflections, and abdominal forces were all reduced somewhat.
- Pelvic forces and accelerations were similar to the conventional restraint.
- ATD rebound excursion was increased somewhat due to a combination of the energy returned by the inflatable restraint and the torque applied to the pelvis by the flailing of the lower legs.
- The lower legs flailed in a similar fashion to the conventional restraint test

Figure A32 - A05074 T = 0

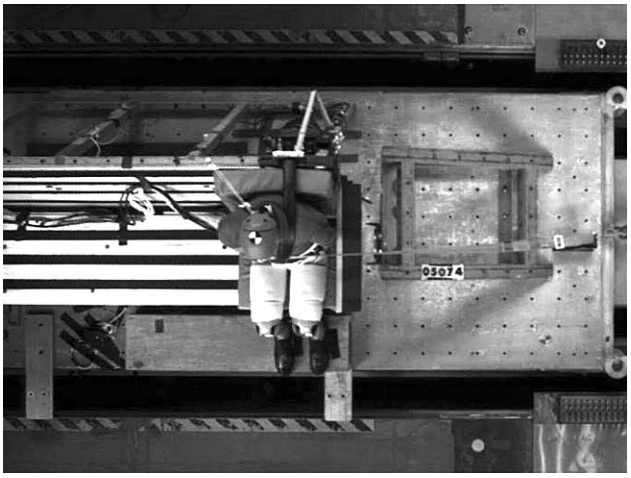

Figure A34 - A05074 (overhead) T = 0

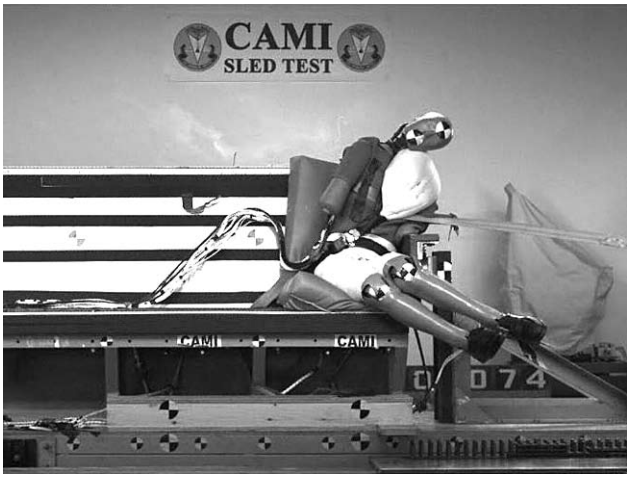

Figure A33 - A05074 T = 158

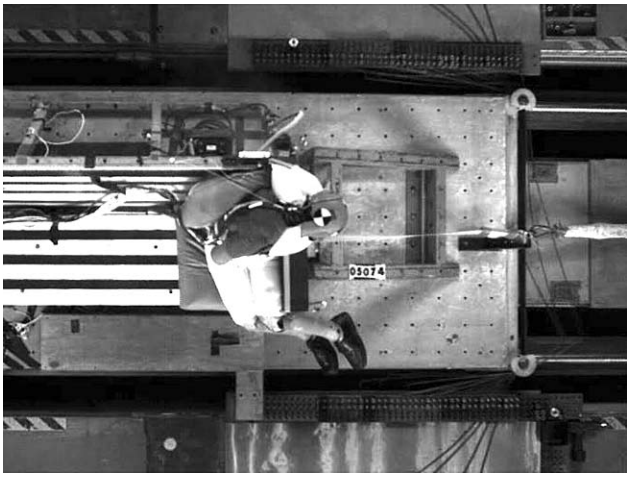

Figure A35 - A05074 (overhead) T = 151

Armrest Configuration – Conventional Restraint –Hybrid III Comparison. (Figures A36 to A39)

- The Armrest Configuration with the conventional restraint was chosen for this comparison test because it provided the greatest overall magnitude of kinematic response.
- The overall kinematics of the H-III were similar to the ES-2 other than the magnitude of the lateral flail envelope.
- There was less lateral excursion than with the ES-2, but a significant amount of lateral flailing still occurred. The 10.5-in length of belt between occupant's shoulder and shoulder belt guide allowed the torso to swing in a combined horizontal and lateral arc that allowed head excursion beyond the armrest and just behind the plane of the seat back. The more rigid load path in the shoulder and chest of the H-III provided a solid reaction surface for the shoulder belt. This is the primary factor that reduced the lateral excursion of the torso.
- The H-III neck is much stiffer laterally than the ES-2. This results in lower forces and moments and lower head excursions and rotation angles. The stiffer compliance of the neck reduces the dynamic overshoot (amplification) of the neck loads. Head motion was reduced to the extent that there was no head impact.
- Shoulder belt forces were nearly half of what was measured with tests using the ES-2. This may be due to differences in the shoulder compliance and geometry between the dummies.
- As with the ES-2 tests, the body-centered lap-belt configuration effectively controlled the lateral excursion of pelvis to the extent that it prevented significant pelvis contact with the armrest. Lap-belt forces were 75% of the forces measured with the ES-2. Pelvic accelerations were similar to the ES-2 tests.
- The left thigh was supported by the armrest resulting in both lower legs flailing in an arc that applied a twisting moment to the femur. The peak measured twisting moment was somewhat higher than measured with the ES-2 and occurred at a lower leg angle. Both the leg-angle time history and the twisting-moment vs. leg-angle plots (A26 and A27) indicate that the H-III femur has a much higher initial torsional stiffness than the ES-2. The biofidelity of this articulation is unknown for either ATD.

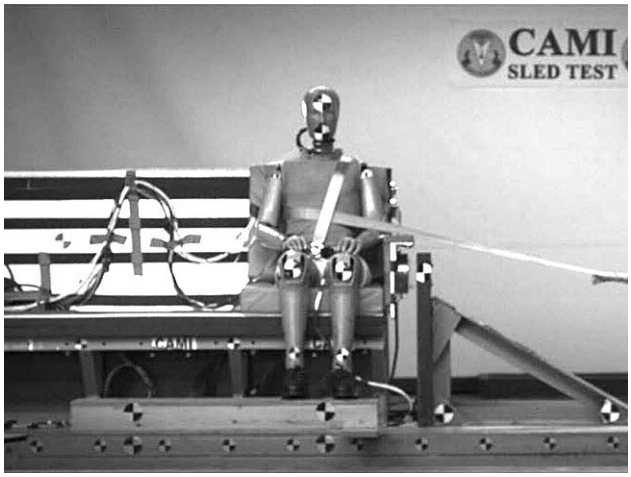

Figure A36 - A06004 T = 0

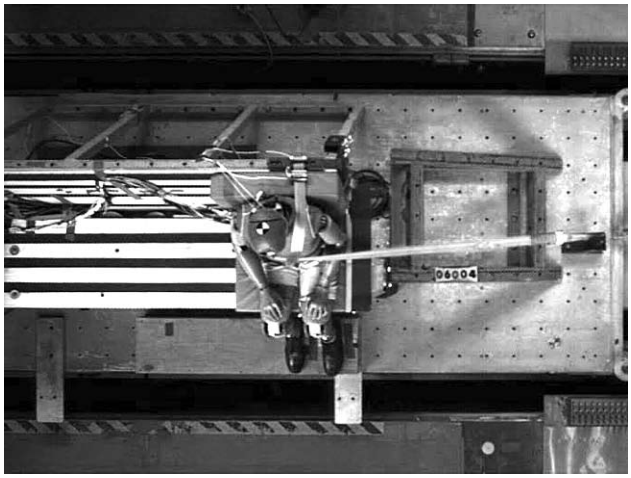

Figure A38 - A06004 (overhead) T = 0

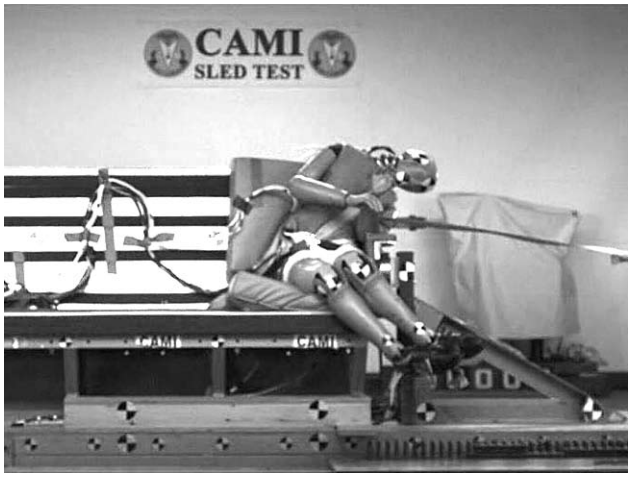

Figure A37 - A06004 T = 160

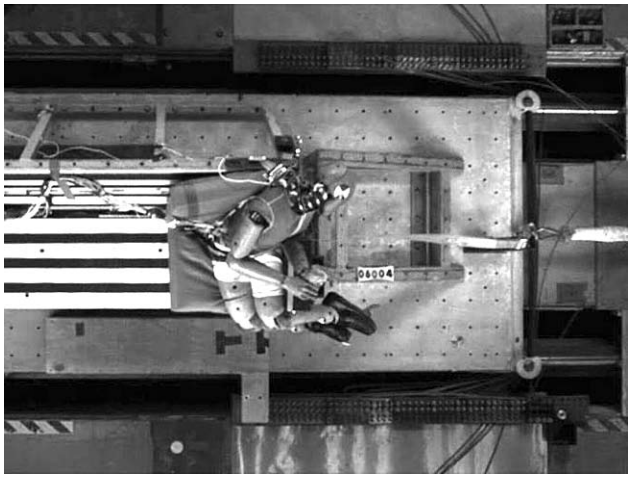

Figure A39 - A06004 (overhead) T = 182